

4-8-2021

Full sequence stress evolution law and prediction model of high stage cemented backfill

Xiao-ming WEI

National Centre for International Research on Green Metal Mining, Beijing 102628, China

Li-jie GUO

National Centre for International Research on Green Metal Mining, Beijing 102628, China,

weixiaoming@bgrimm.com

Xiao-long ZHOU

School of Civil and Resource Engineering, University of Science and Technology Beijing, Beijing 100083, China

Chang-hong LI

School of Civil and Resource Engineering, University of Science and Technology Beijing, Beijing 100083, China

See next page for additional authors

Follow this and additional works at: <https://rocksoilmech.researchcommons.org/journal>



Part of the [Geotechnical Engineering Commons](#)

Custom Citation

WEI Xiao-ming, GUO Li-jie, ZHOU Xiao-long, LI Chang-hong, ZHANG Li-xin, . Full sequence stress evolution law and prediction model of high stage cemented backfill[J]. Rock and Soil Mechanics, 2020, 41(11): 3613-3620.

This Article is brought to you for free and open access by Rock and Soil Mechanics. It has been accepted for inclusion in Rock and Soil Mechanics by an authorized editor of Rock and Soil Mechanics.

Full sequence stress evolution law and prediction model of high stage cemented backfill

Authors

Xiao-ming WEI, Li-jie GUO, Xiao-long ZHOU, Chang-hong LI, and Li-xin ZHANG

Full sequence stress evolution law and prediction model of high stage cemented backfill

WEI Xiao-ming^{1,2}, GUO Li-jie^{1,2}, ZHOU Xiao-long³, LI Chang-hong³, ZHANG Li-xin⁴

1. BGRIMM Technology Group, Beijing 102628, China

2. National Centre for International Research on Green Metal Mining, Beijing 102628, China

3. School of Civil and Resource Engineering, University of Science and Technology Beijing, Beijing 100083, China

4. Anhui Development Mining Co. Ltd., Lu'an, Anhui 237426, China

Abstract: Due to the lack of effective monitoring tools for the slurry flow and strength development of high stage cemented backfill in the metal mines, the conservative design of very high strength of in-situ backfill results in excessive filling costs. The self-designed stress monitoring system were buried horizontally at four sublevels to monitor the temporal and spatial evolution three-dimensional stresses during the full sequence period (filling, curing and bearing). The results indicated that the three-dimensional stresses increased during filling and bearing period but tended to stable during the curing period. Meanwhile, the vertical stress was higher than the horizontal stress at four sublevels. During the filling period, the 51%~65% of self-weight stress was transferred into horizontal stress by the arching effect. The vertical stress and mining distance show a polynomial relationship during the bearing stage. Combined with the second step mining operation process, the mechanism of arching effect and mining-induced stress-transfer was revealed. Based on the double-arch coupling effect of stress transfer, the internal stress prediction model of high stage cemented backfill in the stope was established, which can be used to accurately determine the required strength of backfill.

Keywords: mine backfill; cemented backfill; stress monitoring; double arch coupling; prediction model

1 Introduction

The cemented backfilling method has advantages of improving the recovery rate of mine, reducing the dilution rate, controlling the ground pressure, and reducing the discharge of industrial solid waste, which cannot be replaced by other mining methods^[1–3]. The strength of cemented backfill is the foundation and key of backfill mining design^[4]. The strength design methods of cemented backfill at home and abroad mainly include the empirical method, mechanical model method and numerical analysis method. The empirical method is based on the practical experience of cemented filling in mines to select the strength of cemented filling. Ben et al.^[5] used the real-time monitoring of retaining wall pressure to obtain the variation trend of retaining wall pressure during the filling process, which can guide the strength design at the bottom of mine backfill. Cai et al.^[6] presented an empirical formula of semi-cubic parabola strength design that is based on the statistics of strength design values and filling height of 31 mines at home and abroad. Based on the stress monitoring data of the stope backfill, the physical simulation tests and finite element numerical analysis, the strength of the cemented backfill of Anqing Copper Mine^[7] is determined. In the model method, the mechanical model of backfill is established to derive the required strength value of backfill. There are some widely used models including the Terzaghi

model, Thomas model and Mitchell model etc. In the numerical analysis method, the finite element method, boundary element method or other methods were applied to analyze the contact of the surrounding rock at the filling stope, the distribution of displacement and stress in the surrounding rock and the backfill, so as to predict the required strength of the backfill. Kandiah et al.^[9], Li et al.^[10–13] and Liu et al.^[14] studied the stress distribution of the cemented backfill under exposure and drainage conditions by numerical simulation methods, and proposed the methods for calculation of backfill strength.

At present, the high-stage cemented backfilling method is applied in large domestic metal mines such as Anqing Copper Mine, Dongguashan Copper Mine and Lilou Iron Mine, and the stage height exceeds 90 m^[15]. Due to the lack of effective monitoring methods and theoretical basis for the internal stress of high-stage cemented backfill, the strength and ratio parameters of backfills selected by different mines are subjective, resulting in a large cement–sand ratio and high filling costs. Therefore, based on the engineering background of Lilou Iron Mine, this paper uses a self-developed stress monitoring system to monitor the real-time stress of cemented backfill, and obtains the spatial and temporal evolution of three-dimensional stress in the backfill during the full sequence (i.e., filling phase, curing phase, and bearing phase). By analyzing the

Received: 9 January 2020

Revised: 13 April 2020

This work was supported by the National Key R&D Program of China (2018YFE0123000, 2017YFE0107000) and the Youth Innovation Fund of BGRIMM (04-2027).

First author: WEI Xiao-ming, male, born in 1989, PhD, mainly engaged in the research work of filling body mechanics monitoring and quality evaluation. E-mail: weixiaoming@bgrimm.com

Corresponding author: GUO Li-jie, male, born in 1980, PhD, Professor-level senior engineer, mainly engaged in research work on mine filling technology and resource utilization of mining and metallurgical solid waste. E-mail: guolijie@bgrimm.com

arching effect of high-stage cemented backfill and the transfer mechanism of mining stress, an internal stress prediction model of cemented backfill is established, and the model reliability is further verified.

2 The stress monitoring system of cemented backfills in the stope

The stress monitoring system for cemented backfill is mainly composed of three parts: stress monitoring, data acquisition and data processing software, as shown in Fig.1. The stress monitoring mainly adopts the self-designed and assembled three-way stress monitoring device, see Fig. 2. The measurement range of the VWE vibrating wire stress sensor is 0–4 MPa with the measurement accuracy of $\pm 0.1\%$, and the temperature range is $-20+80\text{ }^{\circ}\text{C}$.

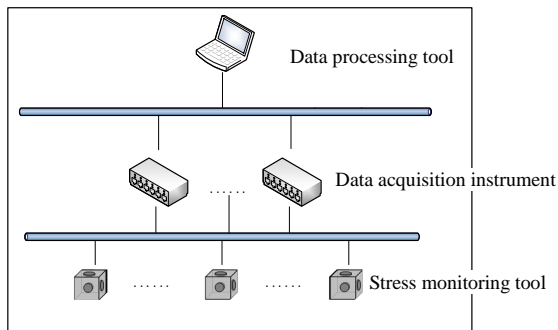
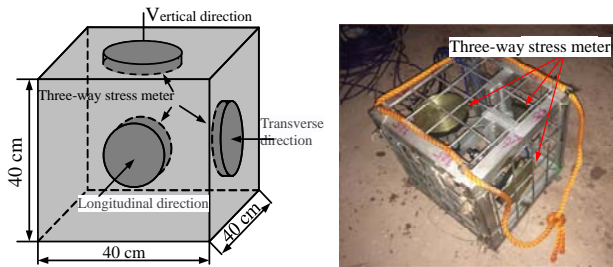


Fig. 1 Stress monitoring system of backfill



(a) Design schematic diagram (b) Measurement system assembled on site

Fig. 2 Design and assembly of stress monitoring system

The MCU-32 distributed data acquisition instrument is used in the real-time stress monitoring of backfill and can store monitoring data in large quantities. MCU-32 consists of one main controller and data acquisition module, as shown in Fig. 3. According to the filling conditions, the sampling interval of the MCU-32 is 20 min.

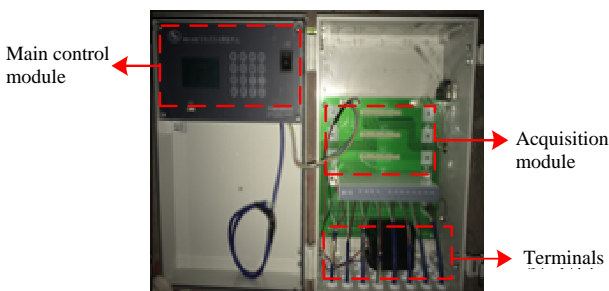


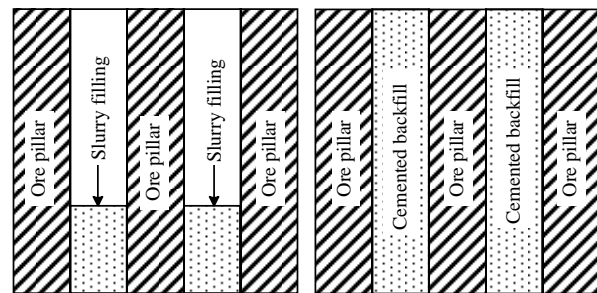
Fig. 3 MCU-32 distributed data acquisition instrument

By analyzing the monitored internal stress of the backfill, the variation trend of internal stress in the backfill can be accurately obtained.

3 Full sequence workflow of cemented backfills in the stope

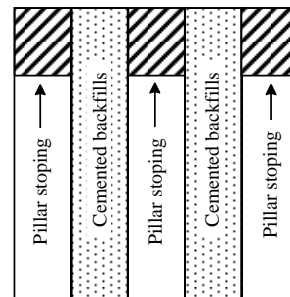
3.1 Full sequence workflow

Lilou iron mine adopts a high-stage cemented backfilling method, with a stage height of 100 m, a sublevel height of 25 m, both the widths of mine room and pillars are 20 m, and the average horizontal thickness of ore body is 50 m. After the first-step mining room is completed, the filling work starts. The full sequence process of cemented backfill in the high-stage stope includes the first-stage slurry filling, the middle-term static curing and the latter bearing stage of cemented backfill, see in Fig. 4.



(a) Slurry filling phase

(b) Static curing phase



(c) Bearing stage

Fig. 4 Full sequence workflow of cemented backfill in the stope

3.2 Stope filling parameters and monitoring point layout

Lilou iron mine adopts the unclassified tailing cemented backfilling process. The aggregate is unclassified tailings, the binder is cemented powder, and the backfill slurry concentration is 71% to 72%. The stope #26-1 of first-step is selected as the test stope, where the -400 sublevel is the ore production level, and the -375 , -350 and -325 sublevels are the rock drilling level. The ratio parameters at 26-1[#] stope are adopted based on the design requirements of 28 days compressive strength R_{28} of the backfill. At the same time, a monitoring point is arranged in each of four segmented horizontal access, as shown in Fig.5.

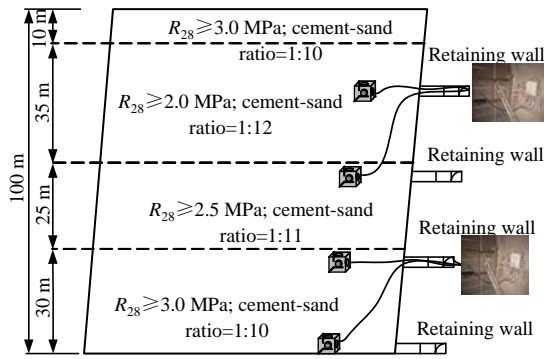


Fig. 5 Ratio parameters of cemented backfill and monitoring layout in the slope #26-1

4 Stress monitoring data analysis

4.1 Full sequence stress monitoring data

After the completion of the slope #26-1 in Lilou iron mine, the installation and commissioning of monitoring instruments were carried out at the design points of the four sublevels at the slope. The test slope started filling on April 7, 2018 and the slope filling was completed on July 11th. The cemented backfill of slope was cured for 3 months. The second-step of slope #24-6 started blasting stoping on October 15, and the blasting stoping was completed on April 11, 2019 (i.e., the bearing stage of cemented backfill at the slope). Through real-time stress monitoring of cemented backfill in the high-stage slope during the full sequence (i.e., filling phase, curing phase and load-bearing phase), as shown in Fig. 6, the temporal and spatial evolution of three-dimensional stress in the cemented backfill can be obtained. Since the test instrument was installed along the slope direction, we set the vertical stress to σ_z , the transverse horizontal stress to σ_x , and the longitudinal horizontal stress to σ_y , the compressive stress was set as "positive", and the tensile stress was set as "negative".

4.2 Stress evolution during the filling stage

4.2.1 Three-dimension

During the filling stage, the 26-1[#] slope was continuously filled for 95 days. With the hydration reaction of cementitious material, the backfill slurry gradually consolidated from the liquid state into a cemented backfill with certain strength and self-supporting ability. It can be seen from Fig. 6 that the three-dimensional stress of slope cemented backfill reaches the peak values with the increase of the height of backfill slurry, and then shows a stable and slightly decreasing trend. The vertical stress is higher than the horizontal stress, and the transverse horizontal stress is higher than the longitudinal horizontal stress. Through the analysis of three-dimensional stress at the four sublevels monitoring points, it can be seen that the vertical stress at the -400 sublevel reaches a peak value of 0.90 MPa when the filling height is 69 m. The new backfill slurry no longer shows an obvious impact on the vertical stress of the backfill. The vertical stress at the -375 sublevel reaches a peak value of 0.65 MPa when the filling height is 74 m. The vertical stress at the -350 sublevel reaches a peak value of 0.33 MPa

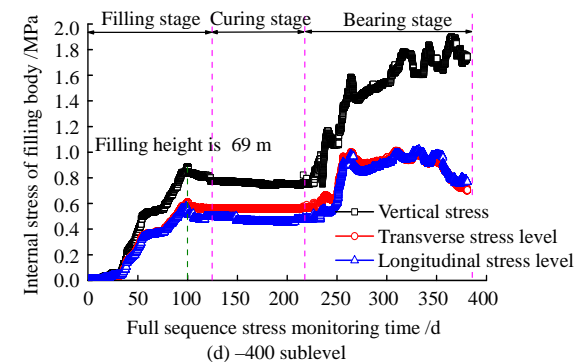
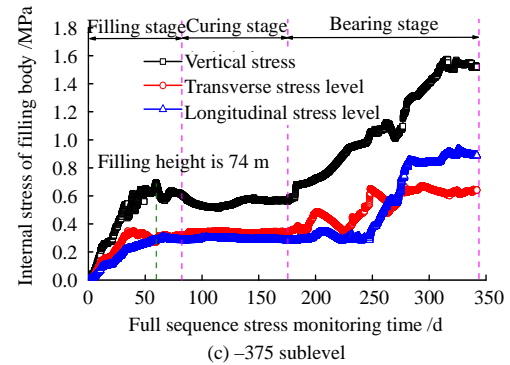
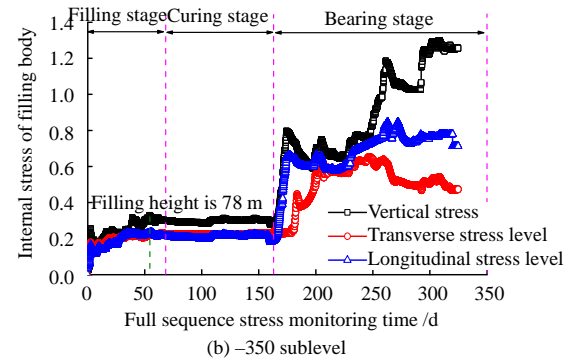
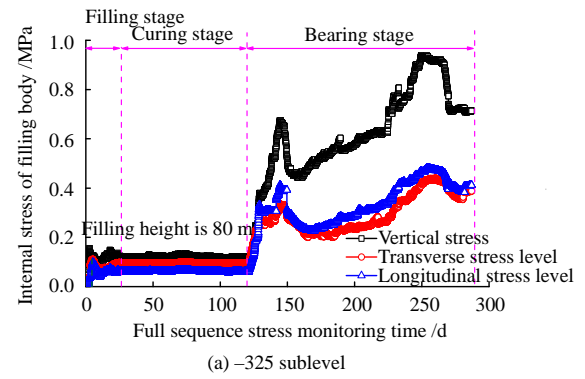


Fig. 6 Full sequence stress monitoring data of cemented backfill

when the filling height is 78 m, while the vertical stress at the -325 sublevel reaches a peak value of 0.16 MPa when the filling height is 80 m.

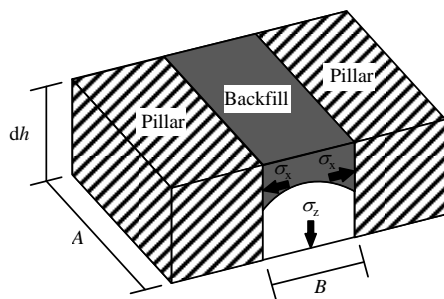
4.2.2 Arching effect analysis

The three-dimensional peak stresses of the cemented backfill in the slope #26-1 are provided in Table 1. The vertical peak stresses of the cemented backfills at four sublevels are 0.16, 0.33, 0.65, and 0.90 MPa, and the gravity stresses are 0.46, 0.92, 1.38 and 1.84 MPa,

respectively. It means that the vertical stress of cemented backfill at the stope is less than the self-weight stress. The main reason is that interfacial friction and cohesion will be produced between the surrounding rocks and the slurry during consolidation after the cemented backfill slurry composed of unclassified tailings enters the stope. Due to the dual effect of interfacial friction and cohesion, the surrounding rock has a certain support on the backfill, resulting in an arch structure in the backfill (see Fig.7), which transfers the vertical stress to horizontal stress of backfill. Under the effect of the stope's lateral sidewall span, the self-weight stress of cemented backfill mainly transfers to the transverse horizontal direction, and the average lateral stress coefficients of transverse horizontal and longitudinal horizontal directions are 0.61 and 0.51, respectively. According to the comparative analysis of vertical stress and self-weight stress of the cemented backfill at the stope #26-1, 51%–65% of the self-weight stress is transferred into horizontal stress through the arching effect. The existence of arching effect greatly reduces the vertical stress of backfill [16].

Table 1 Three-dimensional peak stresses during filling period

Filling height / m	Three dimensional peak stresses /MPa			Horizontal lateral pressure coefficient	
	σ_z	σ_x	σ_y	σ_x / σ_z	σ_y / σ_z
-325	0.16	0.10	0.08	0.63	0.50
-350	0.33	0.22	0.20	0.67	0.60
-375	0.65	0.36	0.28	0.55	0.43
-400	0.90	0.53	0.44	0.59	0.49



A-Length of stope; B-Width of stope; dh-Thin layer height of stope

Fig. 7 Schematic diagram of arching effect of cemented backfill

4.3 Stress evolution of the cemented backfill during curing phase

The cemented backfill at the stope should be cured for 3 months after the filling operation of stope #26-1 is completed, which aims to ensure that the strength of backfill meets the design requirements. In the curing stage of backfill, the three-dimensional stresses of the cemented backfill at the stope shows a steady trend with the increase of the curing age, in which the vertical stress is higher than the horizontal stress, and the transverse horizontal stress is higher than the longitudinal horizontal stress(see Fig.6). Table 2 presents that the average lateral pressure coefficients of transverse horizontal and longitudinal horizontal directions at the four sublevel monitoring points are 0.72 and 0.58,

respectively. It is mainly due to the completion of the internal hydration reaction of cemented backfill at the stope. During the static curing process, the vertical stress of cemented backfill is further transferred to the transverse horizontal direction affected by the arching effect, causing a small decrease in the vertical stress.

Table 2 Three-dimensional peak stresses during the curing period

Filling depth/ m	Three dimensional peak stresses/MPa			Horizontal lateral pressure coefficient	
	σ_z	σ_x	σ_y	σ_x / σ_z	σ_y / σ_z
-325	0.12	0.09	0.06	0.75	0.50
-350	0.30	0.23	0.21	0.77	0.70
-375	0.57	0.34	0.28	0.60	0.49
-400	0.76	0.57	0.48	0.75	0.63

According to the test of unclassified tailings filling ratio, when the slurry concentration is 70% and the curing period is 28 days, the strength of cemented backfill with three different ratios of cement-sand 1:10, 1:11, and 1:12, are 3.33, 2.78, 2.12 MPa, respectively, which meets the design requirements of the strength at the backfill. Because the curing period of cemented backfill at the first-step mining of the -400 sublevel in Lilou iron mine is long, resulting in the stoping lag of the second-step pillar, which seriously affects the connecting progress of two step stopes. Based on the evolution of three-directional stresses during the curing period, the required strength of cemented backfill at the four sub-levels of the stope are 0.12, 0.30, 0.57 and 0.76 MPa, respectively. They are significantly lower than the strength of cemented backfill after 28 days of cured period. Therefore, it is recommended that the **second-step pillar** can be stoped after first-step filling completion and curing for 28 days.

4.4 Evolution of the stress during the bearing phase

With the curing of cemented backfill at the stope #26-1 for 3 months, the blasting stoping was conducted at the second-step pillar stope #24-6. The one-time blasting technology at the medium-deep hole was used at the end of high-stage stope to form a cutting borehole and the cutting slot is regarded as the free surface to blast row by row. When blasting occurs in the sublevel stoping, the upper sublevel is ahead of the lower sublevel by one step of collapse, forming a downward trapezoidal face. It can be seen from Fig. 6 that the internal three-dimensional stresses of cemented backfill in the stope increases with the gradual stoping of two-step stope, and the vertical stress is higher than the horizontal stress. The three-dimensional peak stresses at the four sub-monitoring points are shown in Table 3. The average transverse horizontal and longitudinal horizontal stress coefficients are 0.48 and 0.58, respectively.

Table 3 Three-dimensional peak stresses during bearing period

Filling height/ m	Three-dimensional peak stress/MPa			Horizontal lateral stress coefficient	
	σ_z	σ_x	σ_y	σ_x / σ_z	σ_y / σ_z
-325	0.93	0.42	0.47	0.45	0.51
-350	1.23	0.63	0.83	0.51	0.67
-375	1.57	0.65	0.91	0.41	0.58
-400	1.89	1.01	1.02	0.53	0.54

It is shown from the evolution of three-dimensional stresses during the bearing phase that the redistribution of stress induced by second-step mining is in the cemented backfill, pillar to be mined and surrounding rock of the stope. However, it can be seen from Table 3 that the vertical stress of the cemented backfill in the one-step stope is relatively small, indicating that the bearing capacity of backfill can mainly limit the deformation of surrounding rock in the stope and improve the self-supporting capacity of surrounding rock. The relationship between the vertical stress of first-step cemented backfill and the stoping distance of second-step pillar is shown in Fig. 8. The Origin data analysis software is used to perform polynomial fitting on the scatter plot. The fitting correlation coefficient R_2 at the -325 , -350 , -375 and -400 m sublevels are 0.77, 0.85, 0.95 and 0.94, respectively. The fitting effect is better with the following fitting formula:

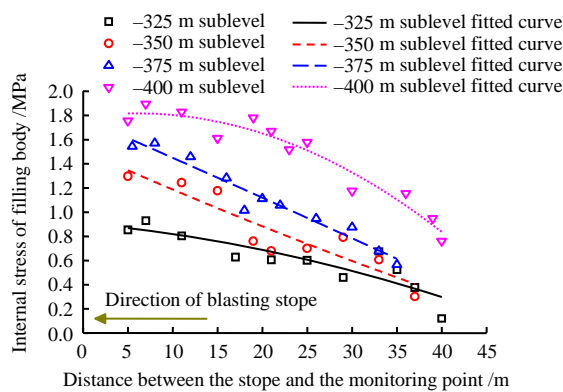


Fig. 8 Variation of vertical peak stress with the stoping distance

$$\sigma_z = \begin{cases} -2 \times 10^{-4} L^2 - 0.0067L + 0.9078 & (-325 \text{ m sublevel}) \\ 9 \times 10^{-5} L^2 - 0.0331L + 1.5087 & (-350 \text{ m sublevel}) \\ -3 \times 10^{-5} L^2 - 0.0322L + 1.7740 & (-375 \text{ m sublevel}) \\ -8 \times 10^{-4} L^2 + 0.0102L + 1.7866 & (-400 \text{ m sublevel}) \end{cases} \quad (1)$$

where L is the distance between the mining face and the monitoring point (m).

4.5 Full sequence stress evolution law analysis

Combined with the three-dimensional peak stress data in Tables 1 to 3, the evolution of three-dimensional peak stresses at the cemented backfill of the 26-1[#] stope during the full sequence (i.e., filling stage, curing stage and bearing stage) is shown in Fig. 9.

(1) In terms of different sublevel heights of cemented backfills in the stope, the three-dimensional stresses at the four segments shows the same evolution trend during the full sequence, indicating that the cemented backfills of high-stage stope are integrated and stable, which have the uniform stress distribution.

(2) The vertical stress is larger in the load-bearing stage than that of the filling stage, followed by the maintenance stage, indicating that the vertical stress of cemented backfill in the stope are mainly divided into

two parts: the self-weight stress in the filling stage and the mining stress in the load-bearing stage. Compared with the filling stage, the vertical stress increments of four sublevels in the load-bearing stage are 0.77, 0.90, 0.92, and 0.99 MPa, respectively. With the gradual mining of second-step ore pillars during the load-bearing stage, it shows that redistribution of ground stress in the mining area occurs because of the roof exposure in the second-step stope when the -325 sublevel stops. Meantime, the vertical stress increase at the one-step cemented backfill is the largest. Afterwards, the one-step cemented backfill is gradually exposed when the mining at the sublevels of -350 , -375 , and -400 m continues. The vertical stress increment is very small in the self-supporting passive support structure.

(3) The horizontal stress during the load-bearing stage is larger than that of the curing stage, followed by the filling stage, which indicates that the horizontal stress of cemented backfill in the stope mainly stems from the arching effect transfer of the vertical stress. The average transverse horizontal pressure coefficients of three stages are 0.61, 0.72, and 0.48, respectively, while the average longitudinal horizontal pressure coefficients are 0.51, 0.58, and 0.58, respectively. In the filling and curing stage, the transverse horizontal pressure coefficient of cemented backfill in the stope is higher than that of the longitudinal horizontal pressure coefficient, indicating that the arching effect is affected by the size of stope during the hydration and consolidation process of backfill, and the vertical stress is mainly transferred to the transverse horizontal stress. In the load-bearing stage, the longitudinal horizontal lateral pressure coefficient of the backfill is higher than that of the transverse horizontal direction, indicating that the arching effect is affected by the exposure of lateral sidewall at the backfill during the two-step stoping process, and the vertical stress is mainly transferred to the longitudinal horizontal stress.

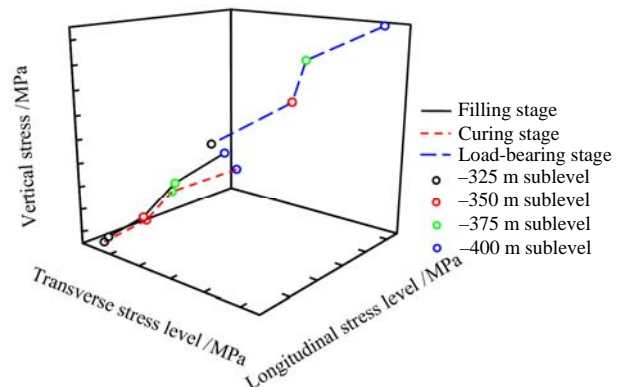


Fig. 9 Evolution of three-dimensional peak stresses during full sequence period

5 Prediction model of internal stress

In order to accurately determine the required strength of cemented backfill in the high-stage stope, it is urgent to establish a internal stress prediction model of cemented backfill. According to the stress evolution

law of in-situ cemented backfill during the full sequence, the vertical stress of backfill mainly results from the self-weight stress in the filling stage and the mining stress in the load-bearing stage. The vertical stress formula is given as follows:

$$\sigma_v = \sigma_a + \sigma_s \quad (2)$$

where σ_v is the full sequence vertical stress of cemented backfill(MPa); σ_a is the vertical stress in the cemented filling stage(MPa); and σ_s is the vertical stress increment in the load-bearing stage(MPa).

During the filling stage, the vertical stress of the cemented backfill in the stope is lower than the self-weight stress due to the arching effect of stope. McCarthy^[17], Aubertin et al.^[18] proposed the vertical stress calculation formula based on the arching effect as

$$\sigma_a(h) = (\sigma_a)_{\max} \left[1 - \exp\left(-\frac{2(h-z)}{B}\right) \right] \quad (3)$$

where B is the width of the stope (m); h is the filling height (m); and z is the location of the monitoring point (m) and $h \geq z$.

After the high-stage stope is filled, the relationship between the vertical stress of cemented backfill and the self-weight stress can be calculated by the following formula:

$$(\sigma_a)_{\max} = \gamma(H_m - z) \frac{H_m}{3(B+L)} \quad (4)$$

where γ is the unit weight of cemented backfill (kN/m³); H_m is the total height of filled stope (m). $z=0$ and $z=H_m$ represent the bottom and top of the stope, respectively.

Substituting Eq. (3) into Eq. (4) leads to

$$\sigma_a(h) = \frac{\gamma(H_m - z)H_m}{3(B+L)} \left[1 - \exp\left(-\frac{2(h-z)}{B}\right) \right] \quad (5)$$

In the load-bearing stage, with the gradual mining of the second-step pillar, the mining stress of the surrounding rock at the pillar roof is redistributed to form an arched pressure bearing zone. Because of the loss of support, the arched overburden touches the cemented backfill after sinking, making it remain in a load-bearing state. When all second-step pillars are mined, each first-step cemented backfill reaches the maximum compression deformation. The pressure-bearing arches of the roofs at two adjacent spaces gradually merge to form a large pressure-bearing arch on the top of the entire mining area. The backfill and the surrounding rock form a mutually mechanical supporting^[19], as shown in Fig. 10. The upper stress reaches the balance, and the radius of the plastic zone in the surrounding rock of roof can be obtained by solving the Kastner equation:

$$\left. \begin{aligned} R_p &= R_0 \left[\frac{(P_0 + c \cot \varphi)(1 - \sin \varphi)}{c \cot \varphi} \right]^{\frac{1 - \sin \varphi}{2 \sin \varphi}} \\ R_0 &= \sqrt{\left(\frac{l}{2}\right)^2 + \left(\frac{h}{2}\right)^2} \end{aligned} \right\} \quad (6)$$

where R_0 is the excavation radius(m); P_0 is the self-weight stress at the excavation location(MPa); φ is the internal frictional angle of the surrounding rock (°); c is the cohesion of the surrounding rock(MPa); and l is the span of the mining space (m).

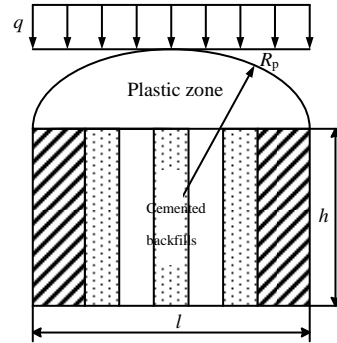


Fig. 10 Bearing mechanism of cemented backfill

The top pressure concentration of cemented backfill in the stope can be estimated by

$$\sigma_b = \gamma_1 \left(R_p - \frac{h}{2} \right) \quad (7)$$

where σ_b is the top pressure concentration of the rock in the plastic zone(MPa); and γ_1 is the unit weight of the surrounding rock at the roof(kN/m³).

The above analysis suggests that the roof of the stope cemented backfill is affected by the compression arch of plastic zone, and the interior of cemented backfill is also affected by the self-arching effect in the load-bearing stage. The internal vertical stress of the cemented backfill is affected by the double-arch coupling effect of stress transfer. Substituting Eq. (7) into Eq. (3) yields

$$\sigma_s(h) = \sigma_b \left[1 - \exp\left(-\frac{2(h-z)}{B}\right) \right] \quad (8)$$

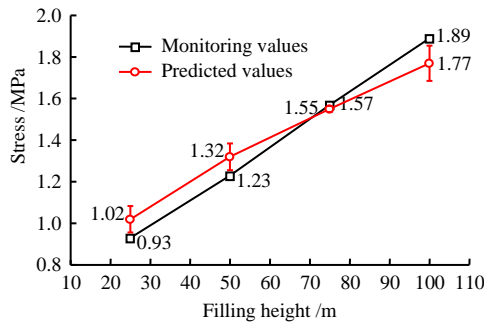
Therefore, the vertical stress of the stope cemented backfill in full sequence is as follows:

$$\sigma_v(h) = \left[\frac{\gamma(H_m - z)H_m}{3(B+L)} + \gamma_1 \left(R_p - \frac{h}{2} \right) \right] \left[1 - \exp\left(-\frac{2(h-z)}{B}\right) \right] \quad (9)$$

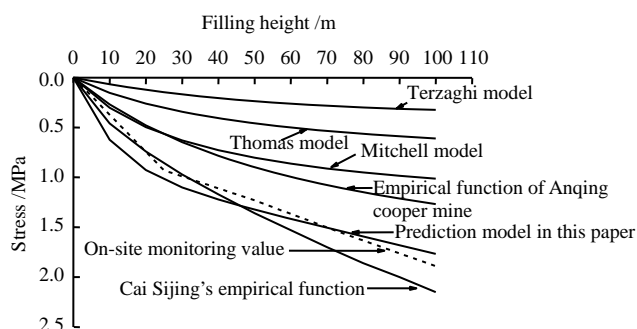
The roof surrounding rock of 26-1[#] stope is muscovite schist. According to the field stress measurement results, the self-weight stress at the -300 sublevel is 10.9 MPa. The parameters of surrounding rock and cemented backfill are given in Table 4. Figure 11 shows the monitoring and model prediction results of the vertical stress at four sublevels of cemented filling in the stope. Based on the standard deviation analysis of the sample data, the standard deviation of overall sample is 0.0568. It shows that the overall discreteness of the data samples between the two is small and the model has a good prediction effect.

Table 4 Mechanical parameters of surrounding rock and cemented backfill

Name	Unit weight/ ($\text{kN} \cdot \text{m}^{-3}$)	Cohesion/ MPa	Internal friction angle/ ($^{\circ}$)	Compressive strength/ MPa
Muscovite schist	27.5	0.97	39	5.68
1:10 backfill	18.3	0.53	42	3.33
1:11 backfill	18.2	0.45	41	2.78
1:12 backfill	18.6	0.28	37	2.12

**Fig. 11 Comparative analysis of monitoring and prediction data of vertical stress at stope #26-1**

The methods for calculating the strength of cemented backfills include Terzaghi model, Thomas model, Mitchell model, Cai Sijing's empirical function, Anqing cooper mine empirical function etc. Combined with the prediction model established in this paper, these 6 kinds of theoretical method are used to calculate the vertical stress at different filling heights of the cemented backfill in the large and tall stope of Lilou iron mine, and the results are presented in Fig.12. Among these six theoretical methods, the calculation results of the Terzaghi model, Thomas model and Mitchell model are significantly lower than that of other theoretical methods, which show a large difference with the field monitoring results, indicating that these three theoretical models have certain limitations. The calculation result based on the empirical formula of Anqing Copper Mine is lower than the in-site monitoring value because the compressive stress of the backfill roof is not considered in the empirical function. The calculation result of Cai Sijing's empirical formula is higher than the in-site monitoring value. The main reason is that the formula only considers the filling height, resulting in a large strength design of the cemented backfill. Based

**Fig. 12 Vertical stress distribution of cemented backfill by six theoretical methods**

on the above analysis, the calculation on the internal stress of the high-stage stope cemented backfill by the prediction model developed in this paper show little dispersion from the field monitoring values. Meanwhile, the prediction model is simple and the parameters are easy to be obtained, making it has a strong applicability.

6 Conclusions

(1) Based on the self-developed three-dimensional stress monitoring system, the real-time stress monitoring of cemented backfill at the 26-1# stope was carried out with full sequence (filling phase, curing phase, and bearing phase). The three-dimensional stresses at the four sub-levels increase first and then stabilize in the filling stage. The horizontal lateral pressure coefficient is 0.43–0.67 and the arching effect transfers 51%–65% of the self-weight stress into horizontal stress. In the curing stage, the three-dimensional stresses at the four sublevels show a steady trend with the horizontal lateral pressure coefficient of 0.49–0.77 and the connection time of two step stopes is 28d. In the load-bearing stage, the three-dimensional stresses at the four sublevels show an increase trend with the horizontal lateral pressure coefficient of 0.41–0.67. The vertical stress and the mining distance shows a polynomial distribution law.

(2) The vertical peak stress at the bearing stage is larger than that of the filling stage, followed by the curing stage, while the horizontal peak stress at the bearing stage is larger than that of the curing stage, followed by the filling stage. Combined with the second-step mining operation process, the arching effect of cemented backfill and the mining stress transfer mechanism is revealed.

(3) Based on the double-arch coupling effect of stress transfer, a internal stress prediction model of cemented backfill in the high-stage stope is established. Compared with the traditional strength theory model, the prediction model is simple, accurate, and the parameters are easy to be obtained, making it has a strong versatility.

References

- [1] JIANG Fei-fei, ZHOU Hui, LIU Chang, et al. Progress, prediction and prevention of rockbursts in underground metal mines[J]. Chinese Journal of Rock Mechanics and Engineering, 2019, 38(5): 956–972.
- [2] WEI Xiao-ming, GUO Li-jie, LI Chang-hong, et al. Study of space variation law of strength of high stage cemented backfill[J]. Rock and Soil Mechanics, 2018, 39(Suppl.2): 45–52.
- [3] YANG Xiao-cong, GUO Li-jie. Comprehensive utilization technology of tailings and waste rock[M]. Beijing: Chemical Industry Press, 2018.
- [4] WU Ai-xiang, SHEN Hui-ming, JIANG Li-chun, et al. Arching effect of long-narrow cemented paste backfill body and its effect on target strength[J]. The Chinese

- Journal of Nonferrous Metals, 2016, 26(3): 648–654.
- [5] BEN D, BRAD B, MURRAY M. Constrained thermal expansion as a causal mechanism for in-situ pressure in cemented paste and hydraulic backfilled stopes[C]//11th International Symposium on Mining with Backfill. Perth: Australian Centre for Geomechanics, 2014: 365–378.
- [6] CAI Si-jing. Mechanics foundation of mine backfill[M]. Beijing: Metallurgical Industry Press, 2009.
- [7] ZHANG Shi-chao, YAO Zhong-liang. Analysis on the stability of fill of extra large stopes in An-qing copper mine[J]. Mining Research and Development, 2001(4): 12–15.
- [8] GUO Guang-li, ZHU Xiao-jun, ZHA Jian-feng, et al. Subsidence prediction method based on equivalent mining height theory for solid backfilling mining[J]. Transactions of Nonferrous Metal Society of China, 2014, 24(10): 3302–3308.
- [9] KANDIAH P, NAGARATNAM S. Arching within hydraulic fill stopes[J]. Geotechnical Geological Engineering, 2007(25): 25–35.
- [10] LI L, AUBERTIN M, BELEM T. Formulation of a three dimensional analytical solution to evaluate stresses in backfilled vertical narrow openings[J]. Canadian Geotechnical Journal, 2005, 42(5): 1705–1717.
- [11] LI L, AUBERTIN M. An improved analytical solution to estimate the stress state in sub-vertical backfilled stope[J]. Canadian Geotechnical Journal, 2008, 45(10): 1487–1496.
- [12] LI L, AUBERTIN M. Influence of water pressure on the stress state in stopes with cohesionless backfill[J]. Geotechnical & Geological Engineering, 2009, 27(1): 1–11.
- [13] LI L, AUBERTIN M. A three-dimensional analysis of the total and effective normal stresses in submerged backfilled stopes[J]. Geotechnical & Geological Engineering, 2009, 27(4): 559–569.
- [14] LIU G S, LI L, YANG X C, et al. Numerical analysis of stress distribution in backfilled stopes considering interfaces between the backfill and rock walls[J]. International Journal of Geomechanics, 2017, 17(2): 1–9.
- [15] LIU G S, LI L, YAO M K, et al. An investigation of the uniaxial compressive strength of a cemented hydraulic backfill made of alluvial sand[J]. Minerals, 2017, 7(1): 1–13.
- [16] WEI Xiao-ming, LI Chang-hong, ZHANG Li-xin, et al. The ratio parameter design and engineering optimization of high stage delayed cemented backfill[J]. Journal of Mining & Safety Engineering, 2017, 34(3): 580–586.
- [17] MCCARTHY D F. Essentials of soil mechanics and foundations: basic geotechnics[M]. New Jersey: Prentice Hall, 1998.
- [18] AUBERTIN M, LI L, ARNOLDI S, et al. Interaction between backfill and rock mass in narrow stopes[J]. Soil and Rock Mechanics America, 2003(2): 1157–1164.
- WEI Xiao-ming. Study on strength characteristics and ratio design of high stage whole tailing cemented backfill[D]. Beijing: University of Science and Technology Beijing, 2018.